Asian Journal of Nanoscience and Materials 5 (2022) 118-131

Asian Journal of Nanoscience and Materials

Journal homepage: www.ajnanomat.com

Original Research Article

Thermodynamic, equilibrium, and kinetic studies of safranin adsorption onto carpobrotus edulis

Abdulfattah Mohammed Alkherraz[a], Khaled Muftah Elsherif[b,*], Abdelmeneim El-Dali[b], Najah A. Blayblo[a], Mohamed Sasi[c]

[a] *Chemistry Department, Faculty of Science, Misurata University, Misurata, Libya*

[b] *Chemistry Department, Faculty of Science, University of Benghazi, Benghazi, Libya*

[c] *Chemistry Department, Faculty of Education, Misurata University, Misurata, Libya*

ARTICLE INFORMATION

Received: 13 March 2022
Received in revised: 9 April 2022
Accepted: 9 April 2022
Available online: 17 April 2022

DOI: 10.26655/AJNANOMAT.2022.2.4

KEYWORDS

Safranin Dye
Adsorption
Kinetics
Isotherms
Thermodynamics

ABSTRACT

In the current study, carpobrotus edulis were used to prepare three adsorbent surfaces; (dry adsorbent material, DAM), (hot activated carbon, HAC), and (acid activated carbon, AAC), and applied for safranin dye removal as a function of pH, contact time, adsorbent dose, initial dye concentration, and temperature. The ideal pH for DAM, HAC, and AAC efficient adsorption were 7-11, 7-9, and 5-11, respectively, employing an adsorbent dosage of 0.10 g and contact time of 30, 40, and 90 min, respectively. Furthermore, the adsorption processes were better explained by the pseudo-second-order-kinetic model. It was also noticed that the safranin adsorption process demonstrated a favorable agreement with Freundlich isotherm for the three adsorbents with maximum calculated adsorption capacities of 47.49, 44.18, and 46.72 mg/g for DAM, HAC, and AAC, respectively. The results of the thermodynamic study revealed the exothermic nature of dye adsorption onto DAM and AAC and the endothermic nature onto HAC. Finally, results demonstrated that the studied surfaces are efficient adsorbents and could likely be utilized for dyes adsorption.

Corresponding author, email: elsherif27@yahoo.com (K.M. Elsherif).
Tel.: 0218923920803.

Graphical Abstract

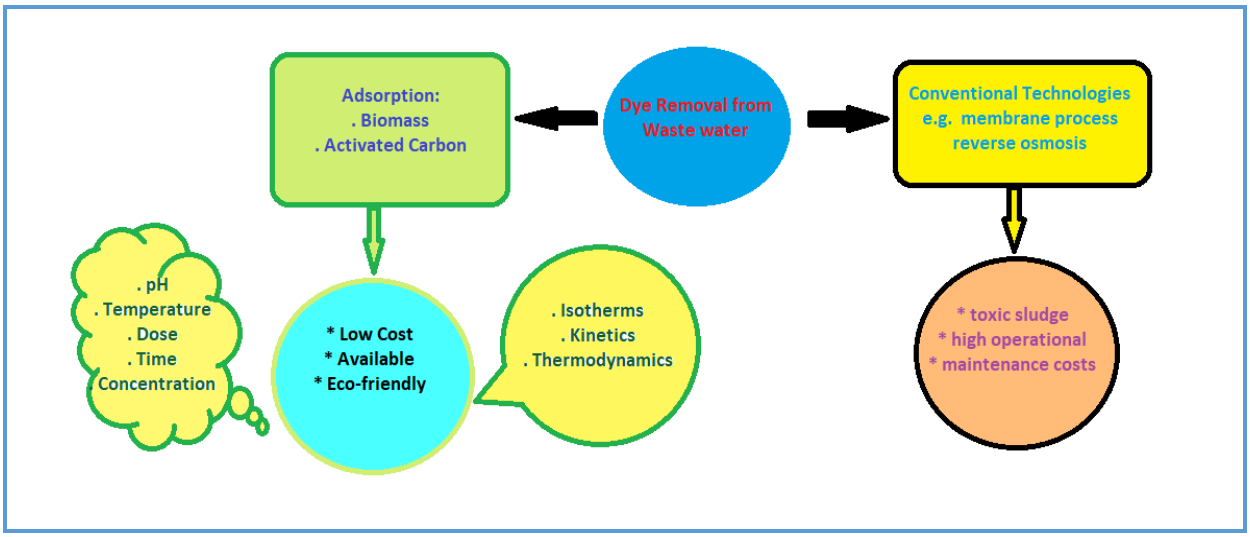

Introduction

Untreated wastewater contains toxic substances, coloring pigments, insoluble substances, acids, and other pollutants such as corrosive substances [1, 2]. Studies have shown that 20% of the dyes produced from the textile, paper, leather, paint, and some pharmaceutical industries are discharged into sewage streams and rivers, which negatively impact the environment and cause health risks to humans [3–5]. These dyes decompose, producing carcinogenic and other toxic substances for living organisms [6, 7]. The difficulty of treating these dyes comes because they are manufactured to be resistant to different environmental conditions such as temperature, light, and pH effects [8, 9]. Dyes are classified as anionic and cationic depending on the ionic charge on the dye molecules [10]. The dye used in this study is O-Safranin, a commonly used azo dye, and it is a cationic dye that is more toxic than anionic dyes [10–16]. O-Safranin is a synthetic dye used in the textile and pharmaceutical industries and is also used to dye cotton, silk, leather, wool, and paper [16]. Although azo dyes are widespread because of their vital and colorful use, they have been regulated due to their toxicity [17]. Whereas clothes containing azo dye are considered to cause cancer when sweating, the study confirmed that O-Safranin dye causes irritation to the respiratory system and can cause infections in the digestive system when ingested [18]. Therefore, it is necessary to remove the concentration of these dyes to the lowest permissible concentration to protect the environment and humans alike. There are various methods for treating wastewater using traditional methods such as sedimentation, ion exchange, and electrochemical processes. Still, they are considered ineffective in effectively removing the dye due to their synthetic composition and complex nature, which are non-degradable [18–25]. The most effective way to remove these dyes from wastewater is through adsorption, which is one of the most effective techniques that have been used successfully to remove dyes from wastewater [26–28]. From the literature survey on safranin adsorption, Kaur *et al.* [29] reported that Tetraethyl orthosilicate (TEOS) and Mesoporous n-cetyl triethyl ammonium bromide (CTAB) surfactant with a size of 6.6-9.8 nm were prepared in a safranin adsorption

experiment using this developed adsorbent, MCM-41.

The adsorption process is well suited by using the second-order reaction rate equation and Langmer's equation. The maximum amount of adsorption was 68.8 mg/g at 303 K. The thermodynamic parameter values were analyzed, and it has been reported as a spontaneous exothermic reaction. Ghaedi *et al*. [30] assessed Fe_3O_4 nanoparticles as a noval adsorbent by studying Safranin-O adsorption using the unmodified Langmuir, Freundlich, Langmuir equations. The competitive modified Langmuir, the expanded, modified Langmuir, because of Freundlich and Sips models, the expanded Freundlich model is the most appropriate. It was found to show an adsorption capacity high is 89.2~91.9 mg/g. Rott *et al*. [31] synthesized MDMLG coated with MgO on multilayer graphene. As a result of the adsorption of Safranin-O, the adsorption equilibrium well meets the Langmuir equation, and the adsorption amplitude was ~3.92×10^{-4} mol/g. The average adsorption energy is ~36.23 kJ/mol. The chemical adsorption process was found to fit well with the pseudo-second-order reaction rate equation.

Moreover, it is possible to regenerate up to 73.5% with ethanol. Shao *et al.* [32] illustrate that more than 90% of Safranin-O can be removed using a nanofiltration membrane using a composite thin film with the operating pressure increase. The removal capacity also increased, and it was good at pH 7~11. This paper reports the preparation of low-cost, active adsorbents prepared from Carpobrotus edulis biomass and its utilization in removing dyes (safranin as a model dye). The effects of various parameters, thermodynamic, equilibrium, and kinetic, on the adsorption process were also investigated.

Experimental

Materials and methods

The dye Safranin ($C_{16}H_{11}N_2O_4SNa$) was purchased from Merck and utilized without further purification. Stock solution of 1000 mg/L concentration was prepared in deionized water and used to prepare dilute solutions with desired concentrations. Deionized water was used for necessary dilutions. Sodium hydroxide concentrated hydrochloric acid, and concentrated phosphoric acid were also purchased from Merck.

Preparation of adsorbent

The Carpobrotus edulis, which had been utilized to prepare three adsorbents in the present study, were collected from a local agricultural area (Misurata-Libya). To prepare dry adsorbent material (DAM), the collected plant was cleaned by carefully washing with double distilled water to eliminate all unwanted particles from the plant and then dried it in sunlight. Then, it was dried in a ventilated oven at 70 °C for about 24 h. After that, the dried material was ground in an electric grinder and sieved to required particle size of <125 μm. Lastly, the dried adsorbent material was stored in storage bottles for further experiments.

The hot and acid-activated carbon adsorbents (HAC and AAC) were prepared by the method described in the literature [33, 34]. The prepared dried material was subjected to pyrolysis at 550 °C in a furnace for 2 h. The formed charcoal was ground into powder, sieved, then rinsed with double distilled water, and finally dried at 60 °C for about 24 h. This material was characterized as hot activated carbon (HAC). The acid-activated charcoal (AAC) was prepared using a portion of the carbonized Carpobrotus edulis charcoal, and 1 M H_3PO_4 was added to it with continuous stirring for 1 h as described elsewhere [34]. Then, the resulted material was diluted with

double distilled water and decanted several times. After that, it was washed with double distilled water until the pH was adjusted to 7. Finally, the acid-activated charcoal was dried in an oven at 110 °C and kept for later experiments.

Analysis of dye

The concentrations of safranin dye before and after the adsorption processes were monitored using a 6305 molecular absorption spectrophotometer from JENWAY at λ_{max}=520 nm. The range of calibration curve concentrations of safranin prepared from the stock solution was between 2-16 ppm. The pH of the solution was measured with a 3505 pH Meter from JENWAY.

Batch sorption studies

Investigation of safranin adsorption onto DAM, HAC, and AAC was carried out using the batch adsorption procedure. Safranin adsorption was studied to demonstrate the effect of several parameters such as pH, contact time, amount of adsorbent, concentration, and temperature. Exactly 0.1 g of adsorbent material was transferred into a series of 150 mL conical flasks with 50 mL safranin solution of different concentrations (5.0-300.0 mg/L) added previously. The pH of each solution was adjusted to 8.0. The prepared conical flasks were positioned in a mechanical shaker at a fixed speed, temperature, and contact time of 150 rpm, 303 K, and 30 min. Finally, the conical flasks were removed at predetermined time intervals, filtered using Whatman filter paper No 1. Then the residual concentration of safranin was determined spectrophotometrically at a wavelength of 520 nm. The safranin removed at equilibrium Q_e (mg/g) was calculated using equation 1. Also, the percentage of adsorbed safranin (%) was calculated using Equation 2 [35, 36]:

$$Q_e = \frac{(C_o - C_e) x\, V}{M} \quad (1)$$

$$\%R = \frac{(C_o - C_e)}{C_o} \text{ x } 100 \quad (2)$$

Where C_o (mg/l), C_e (mg/l), V (l), and M (g) represents the initial safranin concentration, equilibrium safranin concentration, volume of solution, and mass of dried adsorbent material, respectively.

Results and Discussion

Contact time effect and kinetics of adsorption

Contact time influence was investigated from 0 min to 60 min for (DAM, HAC) and from 0 min to 150 min for (AAC), and the results are displayed in Figure 1. Results showed that the contact time significantly influenced the removal of safranin for studied adsorbents (DAM, HAC, and AAC). Furthermore, the removal of safranin dye using DAM and HAC was fast in the first 20 min and slowed down as time advanced, and the equilibrium was established after 30 and 40 min for DAM and HAC, respectively. The maximum removal efficiencies recorded were 98% and 82% for DAM and HAC, at 30 min and 40 min of contact time, respectively. However, safranin adsorption onto AAC was slower and reached equilibrium after 90 min. Subsequently, the optimum contact time for maximum removal of safranin dye was: 30, 40, and 90 min (for DAM, HAC, AAC), and after this time, there was no significant change in adsorption efficiency for the studied adsorbents.

Tables and figures must be embedded in a logical place of the manuscript text to make the work of reviewers comfortable. Figure 1 and Table 1 show illustrative examples. Figures should be inserted in a line, not at a fixed page position to avoid problems in the outlook of the

online-system generated PDF files. If figures or tables contain symbols used for the first time within a manuscript, they must be specified in the legend or footnote.

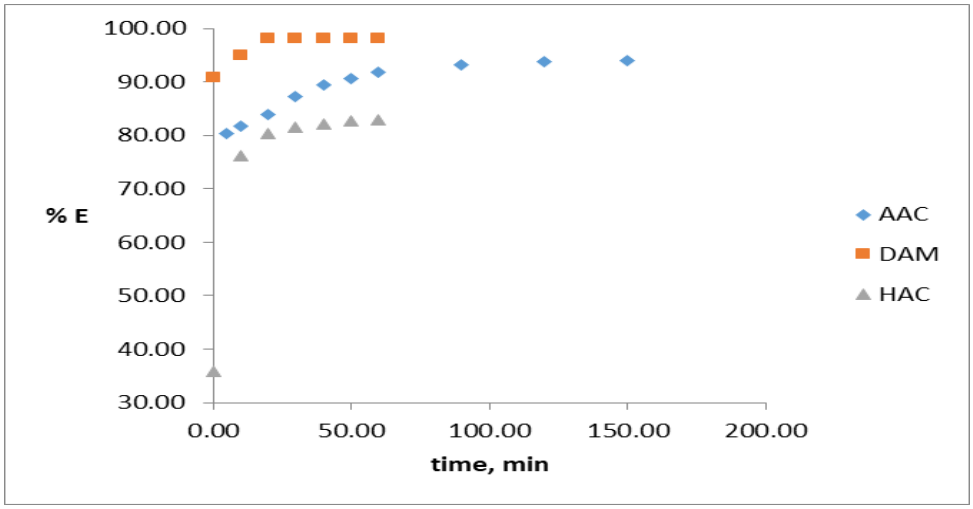

Figure 1. Effect of time on safranin adsorption onto: Carpobrotus edulis (Dry, Hot and Acid activated materials)

Table 1. Kinetic modeling of safranin adsorption onto DAM, HAC, and AAC

Pseudo First Order	K_1 (min^{-1})	Cal. Q_e ($mg.g^{-1}$)	Exp. Q_e ($mg.g^{-1}$)	R^2
DAM	0.0152	0.092	2.46	0.6858
HAC	0.0226	0.810	4.14	0.2767
AAC	0.0223	0.621	2.33	0.6862
Pseudo Second Order	K_2 ($g.mg^{-1}.min^{-1}$)	Cal. Q_e ($mg.g^{-1}$)	Exp. Q_e ($mg.g^{-1}$)	R^2
DAM	6.269	2.458	2.46	1.0000
HAC	1.570	4.189	4.14	0.9979
AAC	0.128	2.467	2.33	0.9976

Pseudo-first-order kinetic model

This model is appropriate to describe the solid/liquid adsorption process. This model illustrates that the change in concentration proceeded as a function of time. The linear equation of pseudo-first-order is expressed in Equation 3 [37, 38]:

$$\text{Log } (Q_e - Q_t) = \text{Log } Q_e - K_1 t \quad (3)$$

where, t is the contact time (min), Q_e and Q_t represent the adsorption capacity (mg/g) at equilibrium and at time t, respectively, while k_1 represents the pseudo-first-order constant (L/min). The K_1 and theoretical Q_e values were evaluated from the slope and intercept of the graph between log (Q_e - Q_t) and t (Figure 2). The values of k_1, coefficient (R^2), calculated, and experimental adsorption capacity (mg/g) are disl-played in Table 1 for examined adsorbents.

Pseudo-second-order kinetic model

The mechanism of adsorption for the whole time range can be realized by successfully applyingthe pseudo-second-order model. The pseudo-second-order differential form is expressed in Equation 4 [39]:

$$\frac{dQ_t}{dt} = K_2(Q_e - Q_t)^2 \quad (4)$$

where, K_2 (g.mg^{-1}.min^{-1}) represents the rate constant. After integration and in the boundary conditions, t = 0 to t = t and Q = 0 to Q = Q_t, the pseudo-second-order linear form is shown in Equation 5:

$$\frac{t}{Q_t} = \frac{1}{K_2 Q_e^2} + \frac{1}{Q_e} t \quad (5)$$

By plotting values of t/Q_t versus t (Figure 3), the values of second-order rate constant K_2 (g·mg–1.min^{-1}) and the theoretical Q_e (mg·g^{-1}) could be calculated using intercept and slope, respectively. The values of K_2, Cal. Q_e, Exp. Q_e and R^2 for safranin removal using DAM, HAC, and AAC are listed in Table 1.

The results elucidated the suitability of the pseudo-second-order model with high values of correlation coefficient (R^2) and the close similarity of experimental and theoretical Q_e values (mg/g) for safranin removal by DAM, HAC, and AAC adsorbents.

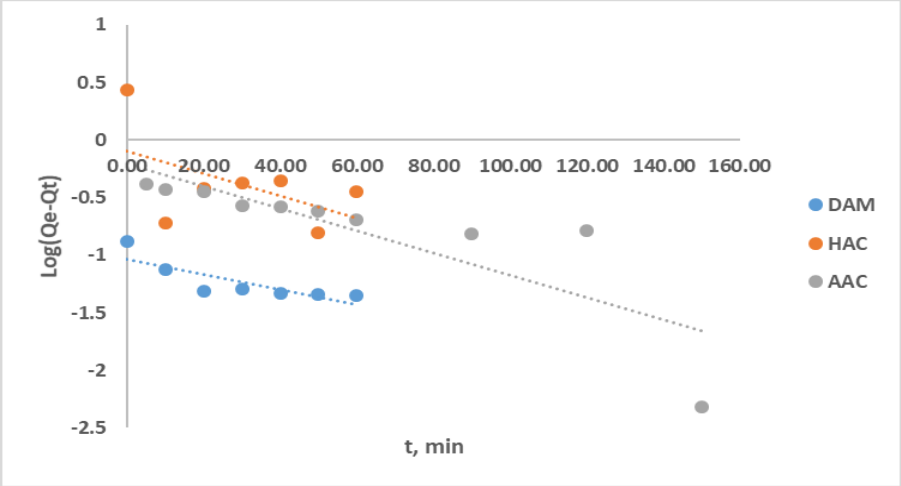

Figure 2. Pseudo first-order kinetic plots for the removal of safranin by adsorption onto Carpobrotus edulis (dry, hot, and acid activated materials)

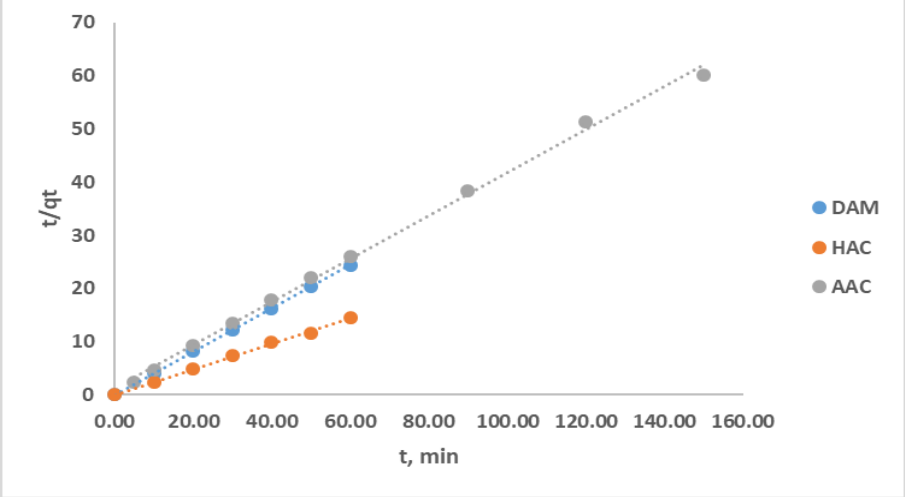

Figure 3. Pseudo-second-order kinetic plots for the removal of safranin by adsorption onto Carpobrotus edulis (dry, hot, and acid activated materials)

Effect of pH

One of the fundamental factors affecting the adsorption of the dye is the pH of the solution. Also, it affects the stabilized structure and color intensity of dye molecules in the solution [40, 41]. Indeed, the critical function of solution pH is to govern the extent of electrostatic charge on both adsorbent surface and dye ions resulting in the variation of solid-phase adsorption capacity for dye molecules [42, 43]. Commonly; at low pH values, the adsorbents favor active uptake of the anionic dye, and at higher pH values, they favor the adsorption of cationic dyes [41]. The alteration of studied adsorbents uptake efficiency (DAM, HAC, and AAC) for the removal of safranin dye was investigated from pH 2 to 13, maintaining the other parameters constant (0.1 g/50 mL adsorbent dose, 25 °C temperature, and 150 rpm and the optimized contact time 30, 40, and 90 min). The obtained results specified that the acidic pH (less than 4) was not appropriate for safranin dye removal (Figure 4). The optimum pH for maximum adsorption efficiency of DAM, HAC, and AAC were established to be 7-11 (95.5%), 7-9 (98%), 5-11 (96%), respectively.

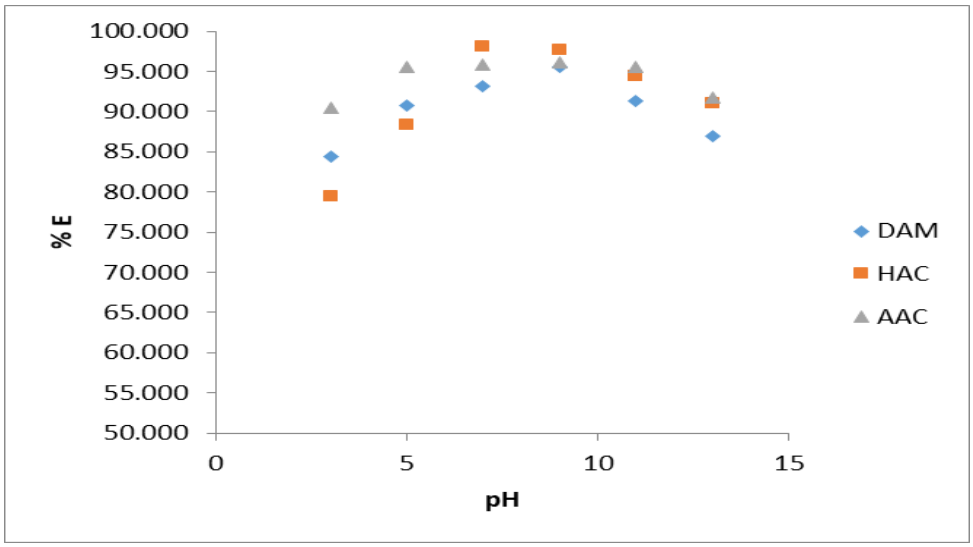

Figure 4. Effect of pH on safranin adsorption onto: Carpobrotus edulis (Dry, Hot and Acid activated materials)

Effect of adsorbent dose

Adsorbent quantity occupies a significant role in the dye adsorption process. The adsorbent dose effect was assessed in 0.05-1.00 g/50 mL of safranin dye solution while maintaining the other parameters constant. The results are displayed in Figure 5. The adsorption capacity of different adsorbents varied with adsorbent dose from 0.05 to 0.50 g. AACDAM, HAC, and AAC adsorption capacity for safranin dye molecules decreased from 9.58 to 0.99 mg/g, 16.06 to 1.89 mg/g, and 18.51 to 2.12 mg/g, respectively. The 0.10 g/50 mL was chosen as an optimum value of adsorbent dose for the maximum removal of safranin dye using the three adsorbents.

Effect of initial dye concentration

Industries discharge wastewater, including various dyes concentrations, and there is a demand to investigate the effect of dye concentration on the adsorption process. Dye

concentration influences adsorption due to the connection between adsorptive sites and dye molecules [44]. As a rule, dye removal efficiency decreased as the concentration increased, which may be due to the saturation of adsorptive sites with dye molecules [40]. When vacant sites on adsorbent become saturated, the adsorption efficiency of dye decreases. Nevertheless, adsorption capacity increases with initial dye concentration, which may be due to the elevated driving force for mass transfer at a higher initial dye concentration [45]. Batch adsorption was utilized to examine the influence of initial dye concentration between 5-1000 mg/L. The other parameters were set as: 0.10 g/50 mL adsorbent dose, 150 rpm shaking speed, and 298 K temperature. The responses are shown in Figure 6. The dye adsorption capacity was increased with dye concentration. The maximum achieved capacity was as follows: 47.49, 44.18, and 46.72 mg/g for DAM, HAC, and AAC, respectively, at 1000 mg/L dye initial concentration.

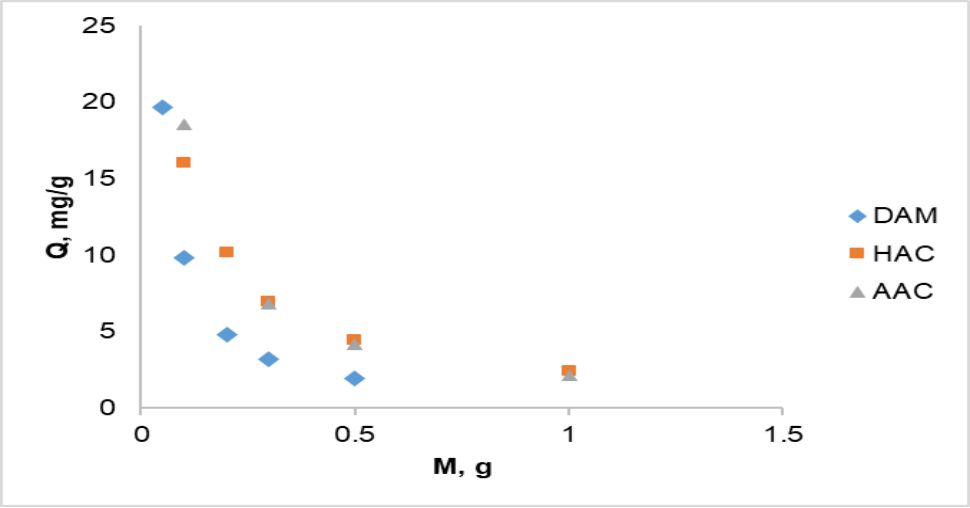

Figure 5. Effect of adsorbent dose on safranin adsorption onto: Carpobrotus edulis (dry, hot and acid activated materials)

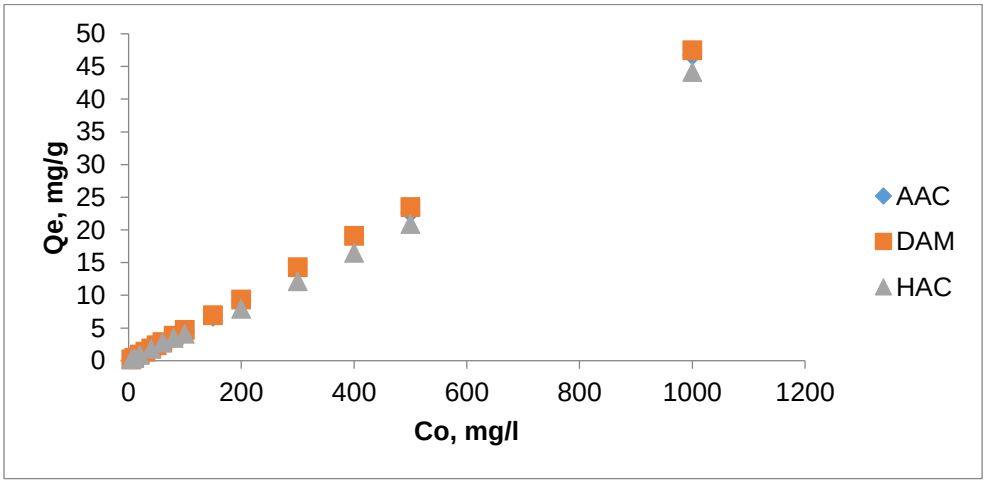

Figure 6. Effect of concentration on safranin adsorption onto: Carpobrotus edulis (Dry, Hot and Acid activated materials)

Isotherm modeling

Langmuir isotherm

As stated by this isotherm model, removing sorbate from the aqueous solution onto the adsorbent surface considered the fixed number of active sites, which establishes monolayer [36, 38, 46]. The linear form of the Langmuir isotherm is displayed in Equation 6.

$$\frac{C_e}{Q_e} = \frac{1}{b\,Q_m} + \frac{C_e}{Q_m} \quad (6)$$

where, Q_m, b and C_e represents the maximum adsorption capacity, Langmuir constant, and dye concentration at equilibrium, respectively. Another Langmuir parameter; R_L, can be evaluated using the relation shown in Equation (7):

$$R_L = \frac{1}{1+b\,C_o} \quad (7)$$

Where, R_L is a unitless quantity and termed equilibrium parameter. C_o and b are dye concentrations at equilibrium and Langmuir constant, respectively. The R_L value establishes the nature of adsorption as; R_L = 0 (reaction is irreversible), R_L = 1 (reaction is linear), and R_L > 1 (unfavorable). The Q_m and b were evaluated from the slope and intercept of the plot between C_e/Q_e and C_e (Figure 7) [36, 38].

Freundlich isotherm

According to the Freundlich model, the removal of dye took place through multilayer formation. It explains the adsorption on a heterogeneous surface having binding sites with different energy contents [36, 38, 47]. The linear expression of the Freundlich isotherm is shown in Equation (8):

$$\text{Log } Q_e = \text{Log } K_f + \frac{1}{n}\text{Log } C_e \quad (8)$$

Where, Q_e and C_e are the adsorption capacity (mg/g) and concentration of dye (mg/L) at equilibrium, while K_f represents the isotherm constant ($mg^{1-(1/n)}$. $L^{1/n}$ g^{-1}) and 'n' is the adsorption intensity. The deviation of adsorption from linearity can be evaluated from n. As n=1 displays the linear adsorption, n<1 reveals the chemical adsorption process, and n>1 represents the favorable adsorption process. The K_f and 'n' were evaluated from the intercept and slope of the relation between the log Q_e versus log C_e (Figure 8), respectively.

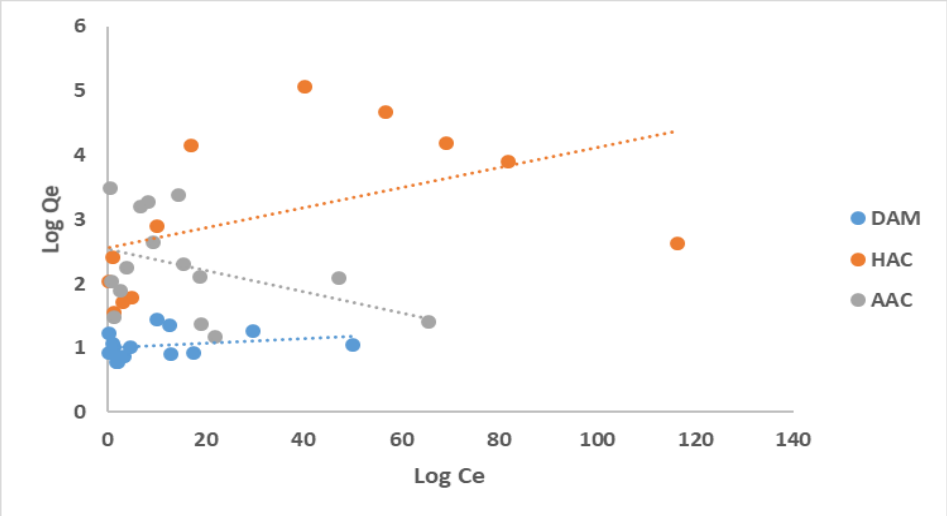

Figure 7. Langmuir adsorption isotherm for the removal of safranin by adsorption onto Carpobrotus edulis (dry, hot and acid activated materials)

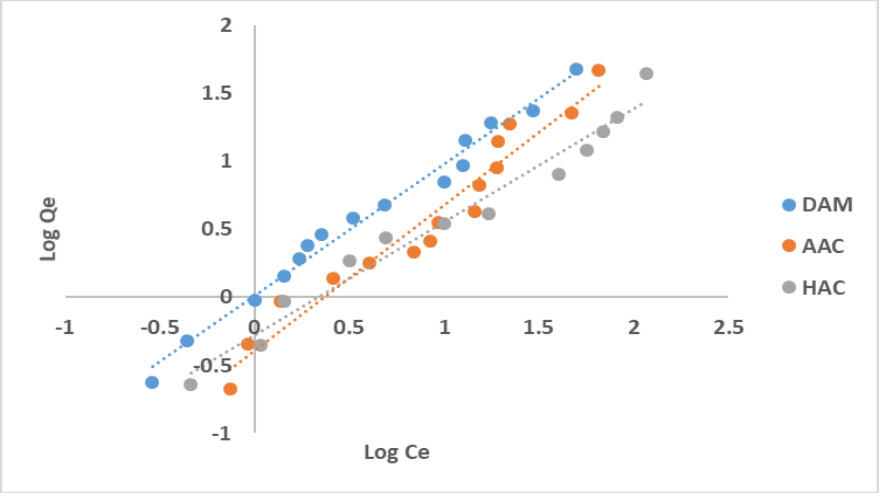

Figure 8. Freundlich adsorption isotherm for the removal of safranin by adsorption onto Carpobrotus edulis (dry, hot, and acid activated materials)

The isotherm models data obtained, correlation coefficient (R^2), calculated, and experimental adsorption capacities (mg/g) for safranin dye adsorption are listed in Table 2. The best fit adsorption isotherm model was selected according to the close agreement of Q_m calculated and experimental values and the R^2. It was noted that the safranin dye adsorption process displayed acceptable fitness for Freundlich isotherms with all adsorbents (DAM, HAC, AAC). The R_L values from the Langmuir model were observed in the range of 0–1, which revealed that the adsorption process for all adsorbents was favorable. The best-fitted model on safranin adsorption was the Freundlich adsorption isotherm with R^2 values: 0.9851, 0.9697, and 0.9493 for DAM, HAC, and AAC, respectively.

Table 2. Equilibrium modeling of safranin adsorption onto three adsorbents

Adsorbent	DAM	HAC	AAC
Freundlich isotherm			
K_f (mg/g (L/mg)$^{1/n}$)	1.028	0.523	0.400
n	1.033	1.200	0.931
R^2	0.9851	0.9697	0.9493
Langmuir isotherm			
b (L.mg^{-1})	0.004	0.006	0.007
Q_m Cal. (mg.g^{-1})	264.41	63.69	60.61
Q_m Exp. (mg.g^{-1})	47.49	44.18	46.72
R_L	0.980-0.200	0.971-0.143	0.966-0.125
R^2	0.0718	0.2409	0.1509

Effect of temperature

The impact of temperature on safranin adsorption was investigated in 25–60 °C while maintaining the other parameters constant. The acquired results are shown in Figure 9. The results presented that the dye adsorption capacity of two adsorbents (DAM and AAC) decreased from 2.47 to 2.33 and 2.15 to 1.65 mg/g, respectively, as the temperature was increased from 30 to 65 °C, which disclosed the

exothermic adsorption process. However, the adsorption capacity of HAC was increased with temperature from 2.35 to 2.43 mg/g, which revealed the endothermic adsorption of safranin onto the HAC adsorbent.

Thermodynamic studies

The thermodynamic parameters like Gibbs free energy change (ΔG), enthalpy change (ΔH), and entropy change (ΔS) were calculated from the data of safranin adsorption for all the three adsorbents using the following equations [24, 27]:

$$\Delta G = \Delta H - T\,\Delta S \quad (9)$$

$$\Delta G = -RT\,\mathrm{Ln}\,K_d \quad (10)$$

where, $K_d = Q_e/C_e$ is the thermodynamic equilibrium constant, R demonstrates the gas constant (8.314 J/mol K), and T (K) represents the absolute temperature. The values of ΔH and ΔS were calculated from the values of slope and intercept by plotting the Ln K_d vs. 1/T (Figure 10) using van't Hoff Equation (11) [27, 37]:

$$Ln\,K_d = \frac{\Delta S}{R} - \frac{\Delta H}{R\,T} \quad (11)$$

The calculated values of thermodynamic parameters are demonstrated in Table 3. For safranin adsorption onto DAM and AAC, the ΔH values were negative; which indicated the exothermic process for the adsorption process. The ΔS values were also negative,, indicating the disorder reduction at the junction of solid and liquid phases during the adsorption process. However, the safranin adsorption onto AAC, the ΔH was positive, which disclosed the endothermic process for the adsorption process, where the ΔS was also positive, which indicates the adsorption process becomes more random. The small and positive ΔG values for safranin adsorption onto HAC and AAC revealed the spontaneous nature of dye adsorption onto these surfaces at low temperatures [48]. However, the negative ΔG for safranin adsorption onto DAM indicated the spontaneous nature of dye adsorption onto the surface at all temperatures.

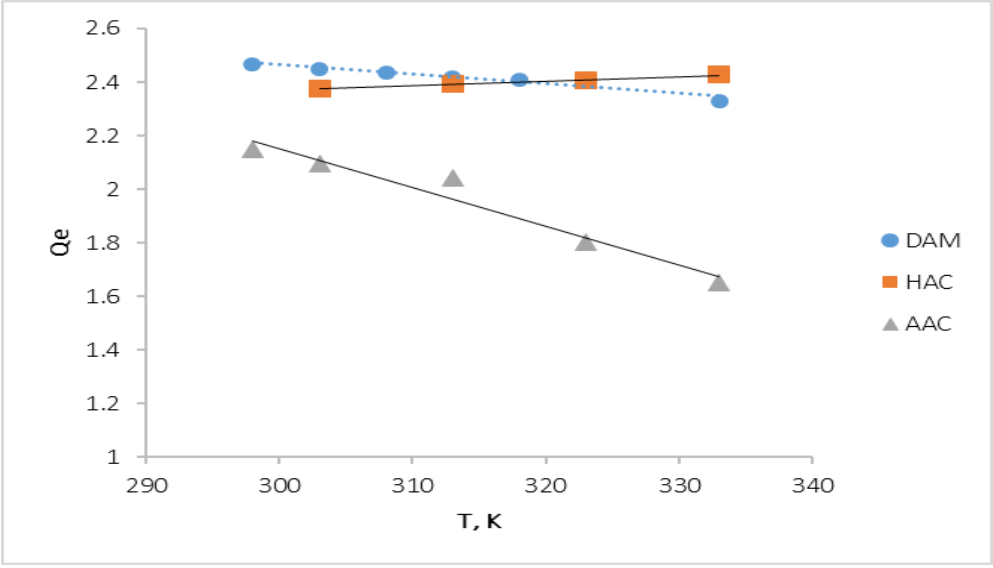

Figure 9. Effect of temperature on safranin adsorption onto Carpobrotus edulis (dry, hot, and acid activated materials)

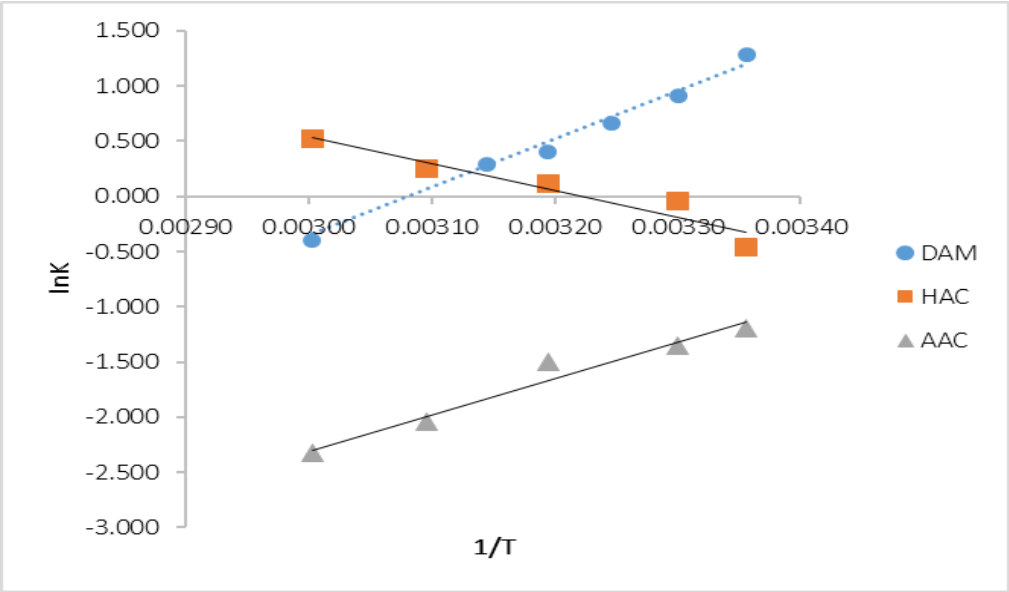

Figure 10. Thermodynamic study of safranin adsorption onto Carpobrotus edulis (dry, hot, and acid activated materials)

Table 3. Thermodynamic parameters of safranin dye adsorption onto the adsorbents at 25 °C

Adsorbent	ΔG^o KJ/mol	ΔH^o KJ/mol	ΔS^o KJ/K.mol	R^2
DAM	-2.84	-36.22	-0.112	0.9695
HAC	0.69	20.06	0.065	0.9131
AAC	2.82	-27.28	-0.101	0.9631

Conclusions

In the present work, three adsorbent surfaces were prepared from Carpobrotus edulis, DAM, HAC, and AAC, and investigated for adsorption of safranin dye from an aqueous solution. The optimum conditions of safranin adsorption realize at pH 7-11, 7-9, and 5-11, at a temperature of 25 °C, and contact times of 30 min, 40 min, and 90 min for DAM, HAC, and AAC, respectively. The maximum adsorption capacities of safranin were 47.49 mg/g, 44.18 mg/g, and 46.72 mg/g for DAM, HAC, and AAC, respectively. The adsorption kinetics and isotherms indicated that the pseudo-second-order, and Freundlich models best presented the adsorption processes. Also, the adsorption process onto DAM and AAC adsorbents was exothermic in nature whears for HAC it was endothermic. Due to the promising adsorption efficiency, the adsorbents have potential as adsorbent and possibly can be used for the remediation of textile wastewater containing dyes.

Disclosure Statement

No potential conflict of interest was reported by the authors.

Orcid

Khaled Muftah Elsherif 0000-0002-3884-1804

References

[1]. Clarke E.A., Anliker R. *Organic dyes and pigments handbook of environmental chemistry, anthropogenic compounds, part A;* Springer-Verlag:New York, 1980; vol. 3; p 181 [Crossref], [Google Scholar], [Publisher]

[2]. El-Hashani A., Elsherif K.M., Edbey K., Alfaqih F., Alomammy M., Alomammy S. *To Chem.*, 2018, **1**:263 [Publisher]

[3]. Mohammed J., Noah U.I., Jibrin I., Madaki K.S., Ingedu Audu S. *Am. J. Phys. Chem.*, 2019, **8**:1 [Crossref], [Google Scholar], [Publisher]

[4]. Elsherif K.M., Yaghi M.M. *Am. J. Ploym. Sci. Technol.*, 2016, **2**:28 [Google Scholar], [Publisher]

[5]. Elsherif K.M., El-Dali A., Alkarewi A.A., Ewlad-Ahmed A.M., Treban A. *Chemistry* International, 2021, **7**:79 [Google Scholar], [Publisher]

[6]. Chiou M.S., Li H.Y. *Chemosphere*, 2003, **50**:1095 [Crossref], [Google Scholar], [Publisher]

[7]. Han R., Ding D., Xu Y., Zou W., Wang Y., Li Y., Zou L. *Bioresour. Technol.*, 2008, **99**:2938 [Crossref], [Google Scholar], [Publisher]

[8]. Ozcan A.S., Erdem B., Ozcan A. *Colloids Surf., A*, 2005, **266**:73 [Crossref], [Google Scholar], [Publisher]

[9]. Sun Q.Y., Yang L.Z. *Water Res.*, 2003; **37**:1535 [Crossref], [Google Scholar], [Publisher]

[10]. Elsherif K.M., Yaghi M.M. Mo*roccan Journal of Chemistry.*, 2017, **5**:131 [Crossref], [Google Scholar], [Publisher]

[11]. Malekbala M.R., Soltani S.M., Yazdi S.K., Hosseini S. *Int. J. Chem. Eng. Appl.*, 2012, **3**: 160 [Crossref], [Google Scholar], [Publisher]

[12]. Sieren B., Baker J., Wang X., Rozzoni S.J., Carlson K., McBain A., Kerstan D., Allen L., Liao L., Li Z. *Adv. Mater. Sci. Eng.*, 2020, **2020**:12 pages [Crossref], [Google Scholar], [Publisher]

[13]. Azimvand J., Didehban K., Mirshokraie S.A. *Adsorpt. Sci. Technol.*, 2018, **36**:1422 [Crossref], [Google Scholar], [Publisher]

[14]. Abdul Hussain A.F., Halboos M.H. *1st International Conference on Pure Science (ISCPS-2020), Journal of Physics: Conference Series*, 2020, 1660 [Crossref], [Google Scholar], [Publisher]

[15]. Elsherif K.M., El-Dali A., Ewlad-Ahmed A.M., Treban A., Alttayib I. *J. Mater. Environ. Sci.*, 2021, **12**:418 [Google Scholar], [Publisher]

[16]. Gupta V.K., Mittal A., Jain R., Mathur M., Sikarwar S. *J. Colloid Interf. Sci.*, 2006, **303**:80 [Crossref], [Google Scholar], [Publisher]

[17]. Brüschweiler B.J., Merlo C. *Regul. Toxicol. Pharmacol.*, 2017, **88**:214 [Crossref], [Google Scholar], [Publisher]

[18]. Ansari R., Mosayebzadeh Z. *J. Iran. Chem. Soc.*, 2010, **7**:339 [Crossref], [Google Scholar], [Publisher]

[19]. Zonoozi M.H., Moghaddam M.R.A., Arami M. 2009. *Water Sci. Technol.*, 2009, **59**:1343 [Crossref], [Google Scholar], [Publisher]

[20]. Ozacar M., Sengil I.A. *J. Hazard. Mater.*, 2003, **98**:211 [Crossref], [Google Scholar], [Publisher]

[21]. Elsherif K.M., Ewlad-Ahmed A.M., Treban A. *World Journal of Biochemistry and Molecular Biology*, 2017, **2**:46 [Google Scholar], [Publisher]

[22]. Elsherif K.M., El-Hashani A., El-Dali A., Saad M. *Int. J. Chem. Pharm. Sci.*, 2014, **2**:890 [Publisher]

[23]. Elsherif K.M., El-Hashani A., El-Dali A. *J. Appl. Chem.*, 2013, **2**:1543 [Google Scholar], [Publisher]

[24]. Alkherraz A.M., Ali A.K., Elsherif K.M. *J. Med. Chem. Sci.*, 2020, **3**:1 [Crossref], [Google Scholar], [Publisher]

[25]. Elsherif K.M., Ewlad-Ahmed A.M., Treban A. *Appl. J. Environ. Eng. Sci.*, 2017, **3**:341 [Crossref], [Google Scholar], [Publisher]

[26] Babel S., Kurniawan T.A. *Chemosphere*, 2004, **54**:951 [Crossref], [Google Scholar], [Publisher]
[27]. Abd El-Salam A.H., Ewais H.A., Basaleh A.S. *J. Mol. Liq.*, 2017, **248**:833 [Crossref], [Google Scholar], [Publisher]
[28]. Elsherif K.M., El-Hashani A., Haider I. *Asian J. Green Chem.*, 2018, **2**:380 [Crossref], [Publisher]
[29]. Kaur S., Rani S., Mahajan R.K., Asif M., Gupta V.K. *J. Ind Eng. Chem.*, 2015, **22**:19 [Crossref], [Google Scholar], [Publisher]
[30]. Ghaedi M., Hajjati S., Mahmudi Z., Tyagi I., Agarwal S., Maity A., Gupta V.K. *Chem. Eng. J.*, 2015, **268**:28 [Crossref], [Google Scholar], [Publisher]
[31]. Rotte N.K., Yerramala S., Boniface J., Srikanth V.V.S.S. *Chem. Eng. J.*, 2014, **258**:412 [Crossref], [Google Scholar], [Publisher]
[32]. Shao L., Cheng X.Q., Liu Ya., Quan S., Ma J., Zhao S.Z., Wang K.Y. *J. Membrane Sci.*, 2013, **430**:96 [Crossref], [Google Scholar], [Publisher]
[33]. Nasuna N., Hameed B.H., Din A.T.M. *J. Hazard. Mater.*, 2010, **175**:126 [Crossref], [Google Scholar], [Publisher]
[34]. Demirbas A. *J. Anal. Appl. Pyrolysis*. 2003, **72**:243 [Crossref], [Google Scholar], [Publisher]
[35]. Alkherraz A.M., Ali A.K., El-Dali A., Elsherif K.M. *To Chem. J.*, 2019, **4**:8 [Publisher]
[36]. Elsherif K.M., El-Hashani A., Haider I. *Iran. J. Anal. Chem.*, 2018, **5**:31 [Publisher]
[37]. Noreen S., Bhatti H.N., Iqbal M., Hussain F., Sarim F.M. *Int. J. Biol. Macromol.*, 2020, **147**:439 [Crossref], [Google Scholar], [Publisher]
[38]. Elsherif K.M., Haider I., El-Hashani A. *J. Fundam. Appl. Sci.*, 2019, **11**:65 [Google Scholar], [Publisher]
[39]. Ho Y.S. *J. Hazard. Mater.*, 2006, **136**:681 [Crossref], [Google Scholar], [Publisher]
[40]. Tahir M.A., Bhatti H.N., Hussain I., Bhatti I.A., Asghar M. *Z. Phys. Chem.*, 2019, **234** [Crossref], [Google Scholar], [Publisher]
[41]. BhattiH.N., Jabeen A., Iqbal M., Noreen S., Naseem Z. *J. Mol. Liq*., 2017, **237**:322 [Crossref], [Google Scholar], [Publisher]
[42]. Nisar N., Ali O., Islam A., Ahmad A., Yameen M., Ghaffar A., Iqbal M., Nazir A., Masood N. *Z. Phys. Chem.*, 2019, **233** [Crossref], [Google Scholar], [Publisher]
[43]. Shoukat S., Bhatti H. N., Iqbal M., Noreen S. *Micropor. Mesopor. Mater.*, 2017, **239**:180 [Crossref], [Google Scholar], [Publisher]
[44]. Ata S., Tabassum A., Bibi I., Ghafoor S., Ahad A., Bhatti M. A., Islam A., Rizvi H., Iqbal M. *Z. Phys. Chem.*, 2019, 1203 [Crossref], [Google Scholar], [Publisher]
[45]. Tahir M. A., Bhatti H. N., Iqbal M. *J. Environ. Chem. Eng.*, 2016, **4**:2431 [Crossref], [Google Scholar], [Publisher]
[46]. Langmuir I. *J. Am. Chem. Soc.*, 1918, **40**:1361 [Crossref], [Google Scholar], [Publisher]
[47]. Freundlich H. *Colloid Polym. Sci.*, 1912, **11**:257 [Google Scholar], [Publisher]
[48]. Duran M., Arar ö., Arda M. *J. Chil. Chem. Soc.*, 2019, **64**:4399 [Google Scholar], [Publisher]

How to cite this manuscript: Abdulfattah Mohammed Alkherraz, Khaled Muftah Elsherif*, Abdelmeneim El-Dali, Najah A. Blayblo, Mohamed Sasi. Thermodynamic, equilibrium, and kinetic studies of safranin adsorption onto carpobrotus edulis. *Asian Journal of Nanoscience and Materials*, 5(2) 2022, 118-131. DOI: 10.26655/AJNANOMAT.2022.2.4